Arabian Journal for Science and Engineering (2019) 44:1243–1253
https://doi.org/10.1007/s13369-018-3477-7

RESEARCH ARTICLE - MECHANICAL ENGINEERING

Microstructural and Mechanical Evolution of Semisolid 7075 Al Alloy Produced by SIMA Process at Various Heat Treatment Parameters

Ali Tekin Guner[1] · Derya Dispinar[2] · Engin Tan[3]

Received: 29 May 2018 / Accepted: 19 July 2018 / Published online: 1 August 2018

Abstract
A homogeneous equiaxed grain structure is necessary for semisolid forming of aluminum alloys. One of the methods used to obtain such microstructure is strain induced melt activated process. The aim of this work is to optimize the heat treatment parameters for extruded 7075 alloy required to obtain the spheroidal grain structure suitable for thixoforging. For this purpose, 7075 was subjected to isothermal heat treatment at two different temperatures, 620 and 630 °C for 5, 10, 15, 20, 25, 30, 35 and 40 min. Optical microscopy analysis and mechanical tests were carried out to characterize the effects of different isothermal heat treatment parameters. Optimal heat treatment parameters were determined by the change in mechanical properties and microstructure. It was found that at 630 °C for 25 min resulted in 564 MPa yield stress, 616 MPa tensile stress and 5.3% elongation as the highest values in the experimental work carried out in this study.

Keywords SIMA · Semisolid · Isothermal · Heat treatment · 7075

1 Background

The 7xxx series aluminum alloys are widely used in automotive and aerospace industries due to high specific strength, corrosion resistance and low cost [1–8]. Most widely used methods for the manufacture of aluminum alloy components are casting in liquid state and forging in solid state. Main disadvantages of casting are shrinkage due to liquid/solid density difference, requirement for feeder and runner calculation, porosity formation and non-uniform material properties [9]. On the other hand, net-shape methods such as forging can result in superior mechanical properties; no need for a runner or feeder [10]. However, it is impossible to work with thin sections and complex geometries. Additionally, very high pressures and consequently high mold costs are required. Semisolid forming is a relatively novel manufacturing method which combines the advantages of forging and casting [9,11,12].

Semisolid forming methods can be categorized into two main routes as indirect processes and direct processes which is determined by the process as it is carried out intermittently or continuously (Fig. 1) and according to another classification, two groups as rheoforming and thixoforming. In thixoforming processes, the metal which is completely solid at the beginning of the process is shaped like forging or poured like casting by heating to a semisolid temperature. In rheoforming processes, the metal which is completely liquid at the beginning of the process is shaped or poured by cooling to a semisolid temperature.

A fine homogeneous equiaxed spheroidal grain structure is necessary to form aluminum alloys in semisolid state without the formation of tears or cracks because the dendritic structure exhibits great resistance to fluidity [13], and spheroidal microstructure has better mechanical properties than dendritic microstructure [14]. One of the methods used to obtain this microstructure is SIMA (Strain Induced Melt Activated) process. In this process, after casting, the material is first subjected to hot deformation by a method like extru-

✉ Engin Tan
etan@pau.edu.tr

Ali Tekin Guner
alitekinguner@pau.edu.tr

Derya Dispinar
deryad@istanbul.edu.tr

[1] Department of Automotive Engineering, Faculty of Technology, Pamukkale University, Denizli, Turkey

[2] Department of Metallurgical and Materials Engineering, Faculty of Engineering, Istanbul University, Istanbul, Turkey

[3] Department of Metallurgical and Materials Engineering, Faculty of Technology, Pamukkale University, Denizli, Turkey

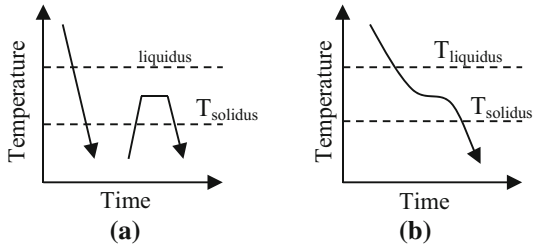

Fig. 1 Indirect (**a**) and direct (**b**) semisolid forming processes

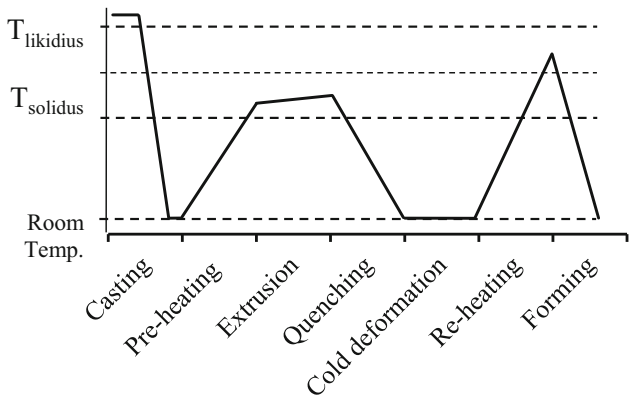

Fig. 2 Steps and temperature ranges of SIMA process [15]

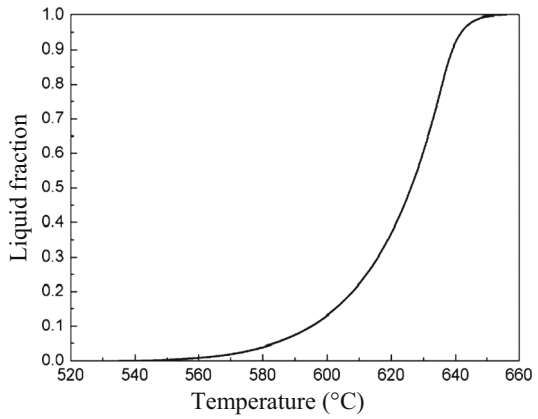

Fig. 3 Liquid volume rate of 7075 aluminum alloy versus temperature [16]

sion or rolling to obtain a heavily deformed structure with increased dislocation density. Spheroidal grains are obtained by recrystallization during reheating of the alloy to a suitable temperature in the liquidus-solidus range (Fig. 2).

7075 alloy's wide freezing range between 477 and 635 °C makes this alloy suitable for semisolid forming applications. According to Fu et al. [16], the evolution of liquid volume fraction in 7075 alloy with increasing temperature is illustrated in Fig. 3.

Chayong et al. [17] and Rikhtegar and Ketabchi [18] reported that yield strength and elongation values close to those of wrought 7075-T6 alloy are obtained with thixoforming followed by T6 heat treatment. Atkinson et al. [12] reported that fully spheroidal microstructures were obtained by isothermal heat treatment of wrought 7075-T6 alloy at about 580 °C with 5% liquid fraction. Sang-Yong et al. [19] suggested a minimum of 50% cold deformation and isothermal heat treatment at 590 °C at for 30 s to 3 min for thixoforming of 7075 alloy and according to Bolouri et al. [20] 30% compression ratio and at least 10 min at 610 °C is needed to obtain optimum grain size and uniform spheroidal microstructure. Neag et al. [21] observed that the grains of 7075 alloy transformed into a much more equiaxed spheroidal structure after 15–20 min isothermal heating at 580 °C and the structure altered to an irregular polygonal shape with smoother and faceted boundaries with some solid grains surrounded by liquid phase after 30 min. In the study of Binesh and Aghaie-Khafri [22], isothermal heating at 600–610 °C for 15–25 min is suggested as optimum parameters for the SIMA process to obtain desired material properties in cold deformed 7075 alloy. Jiang et al. [23] stated that higher isothermal temperature led to shorter spheroidization time and optimal isothermal treatment time of 20 min was suggested for RAP and SIMA processes in 7075 alloy. Meshkabadi et al. [24] concluded that the most suitable microstructure was obtained by heating at 630 °C for 15 min in semisolid 7075 alloy. Li et al. [25] reported that the suitable melt treatment temperature is between 680 and 690 °C for the semisolid A356 aluminum alloy in rheological forming. Zhou et al. [26] suggested that with the increasing stirring speed, mean grain size decreases and the shape factor as well as the number of primary grains increase in forced convection rheoforming process of 7075 alloy. Kilicli et al. [27] observed that T6 treatment with prolonged solution treatment significantly improved the tensile properties of the thixocast 7075 alloy. Yan et al. [28] stated that average particle size gradually decreases and the degree of spheroidization improves with the increasing compression ratio in A356.2 alloy prepared by the SIMA process. Mohammadi et al. [29] reported that higher semisolid isothermal temperature increases the liquid volume fraction and accelerates the spherical evolution of the solid particles and longer holding times increases the average grain size. Gecu et al. [30] investigated influence of T6 heat treatment on A356 and A380 alloys manufactured by thixoforging combined with low superheat casting. Spheroidal structure of α(Al) disappeared and deformation texture was observed after thixoforging, and the grain growth by increasing reheating time caused a decrease in mechanical properties.

This section has attempted to provide a brief summary of the literature relating to semisolid forming of 7075 alloy. Different isothermal heating times and temperatures have

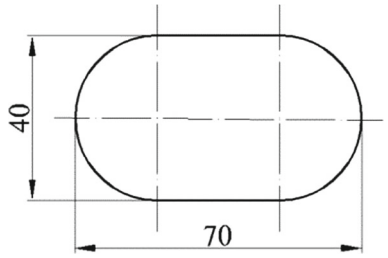

Fig. 4 7075 alloy rod dimensions used in the study

been used for various applications. In some studies grain size, form factor and solid fraction which are fundamental parameters that are of great importance for semisolid forming have not been fully investigated while some investigated the microstructural evolution but the changes in mechanical properties and the mechanical properties after precipitation hardening were not addressed. In this study, isothermal heat treatment was applied at a higher temperature range than previous studies for a shorter holding time and optimum temperature and holding time parameters were selected by examining grain size, form factor and solid fraction parameters together. Furthermore, the specified parameters were supported by hardness and tensile tests and a relationship between spheroidization, liquid fraction, grain size and processing time with mechanical properties was stated. In addition, 7075 alloy with spherical microstructure is subjected to precipitation hardening heat treatment to assess the effect of isothermal heat treatment on the mechanical properties of the wrought 7075-T6 alloy.

The purpose of the present work is to evaluate the effect of holding temperature and duration on the microstructural and mechanical properties of a semisolid 7075 alloy during the reheating process and to present optimum heat treatment parameters for extruded 7075 alloy in order to obtain the equiaxed spheroidal grain structure with suitable solid/liquid ratio for thixoforging applications.

2 Material and Methods

For the present study, 7075 alloy rod-shaped material (Fig. 4) produced by extrusion and subsequent stretching to straighten and impart cold work to the extrusion was provided from Al Metal Aluminum Industry and Trade Inc. in Seydisehir/Konya/Turkey.

The chemical analysis of 7075 alloy examined in this article is shown in Table 1.

Different isothermal heat treatment parameters have been determined in order to assess the effects of isothermal heat treatment temperature and times required to obtain homogeneous spheroidal grain structure within the SIMA process.

Table 1 Chemical composition of 7075 alloy examined in the tests (%)

Al	Zn	Mg	Cu	Fe	Si	Cr
90.3	5.08	1.97	1.21	0.5	0.26	0.23
Mn	Zr	Ni	Ti	Pb	Sn	
0.21	0.04	0.04	0.02	0.02	0.018	

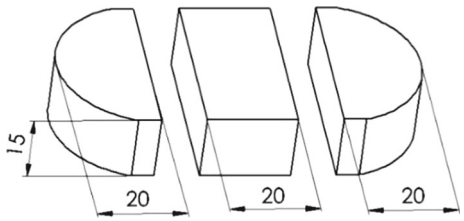

Fig. 5 Heat treatment samples

Table 2 Etching solutions

Etchant	Ingredients
Keller's	5 ml of nitric acid (HNO_3), 3 ml of hydrochloric acid (HCl), 2 ml of hydrofluoric acid (HF), 100 ml of distilled water (H_2O)
Weck's	4 g of potassium permanganate ($KMnO_4$), 1 g of sodium hydroxide (NaOH), 100 ml of distilled water (H_2O)
%10 NaOH	10 g of sodium hydroxide (NaOH), 100 ml of distilled water (H_2O)
Graff & Sargent's	15.5 ml of nitric acid (HNO_3), 0.5 ml of hydrofluoric acid (HF), 3 g of chromium-III-oxide (Cr_2O_3), 84 ml of distilled water (H_2O)
Macro	5 ml of hydrofluoric acid (HF), 20 ml of hydrochloric acid (HCl), 20 ml of nitric acid (HNO_3), 60 ml of distilled water (H_2O)

Temperature was selected as 620 and 630 °C, while the duration was selected as 5, 10, 15, 20, 25, 30, 35, 40 and 45 min.

The samples were prepared by machining the bars as shown in Fig. 5. Metallographic samples were prepared according to ASTM E3-11 (2017) standard. The heat-treated samples were cut perpendicular and parallel to the extrusion direction, then ground with 320, 1100 and 2400 grit SiC abrasive papers and then polished with a 3 μm diamond solution.

Table 2 gives the etching solutions and chemical compositions tried to investigate microstructure of 7075 alloy. Grain size, shape factor and liquid fractions were determined by quantitative image analysis with SPIP^{TM} (version 6.7.2) digital image processing software. Grain size is determined by calculating the diameter of a circle having an area equal to the area enclosed by the grain's contour (Eq. 1). Shape factor describes the sphericity in accordance with Eq. 2 where a

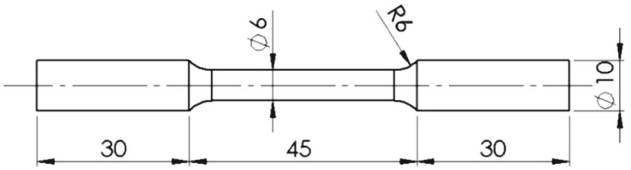

Fig. 6 Tensile test specimen dimension

perfect circle would have a shape factor of 1. Approximately 500 grains were measured for the analysis.

$$\text{Diameter} = \sqrt{\frac{4}{\pi}\text{enclosed area}} \quad (1)$$

$$\text{Shape factor} = \frac{4.\pi.\text{area}}{\text{perimeter}^2} \quad (2)$$

After isothermal heat treatment, T6 tempering treatments were carried out with the following steps: solutionizing at 490 °C for 45 min, immersing in water at 20 °C and artificial aging at 120 °C for 48 h.

T6 tempered specimens were machined into cylindrical tensile test specimens (Fig. 6). Tensile tests were practiced in accordance with ASTM E8/E8M-16a. Brinell hardness test were carried out after each heat treatment according to ASTM E10-17.

3 Results and Discussion

Figure 7 shows the optical micrographs of the samples etched with different solutions. The most common etchant for aluminum alloys is Keller's Solution, but the grain structure of the extruded samples without isothermal heat treatment could not be visualized with Keller's solution. Therefore, the etching solutions in Table 2 were tested and Weck's Solution was selected as the most appropriate etchant for extruded samples without isothermal heat treatment. The grain structure of the sample subjected to 25 min of isothermal heat treatment at 630 °C could be visualized by etching with both Keller's and Weck's solutions. But the Keller's solution exposes grain boundaries more clearly and appropriately for digital image analysis. The heat treatment condition of the material is an important factor for etchant selection.

Microstructure of the initial extruded and stretched specimen without isothermal heat treatment includes intermediate phases (bright zones) and elongated Al grains (dark zones) (Fig. 7a, b). It is seen that the dendrite arms formed during casting are mostly broken in perpendicular direction to the extrusion direction, and in the case of the section parallel to the direction of extrusion, grains are elongated to a great extent in the direction of extrusion. According to Zhang et al. [31], internal strain energy is stored as multiplication of dislocations, elastic stresses and vacancy defects during the plastic

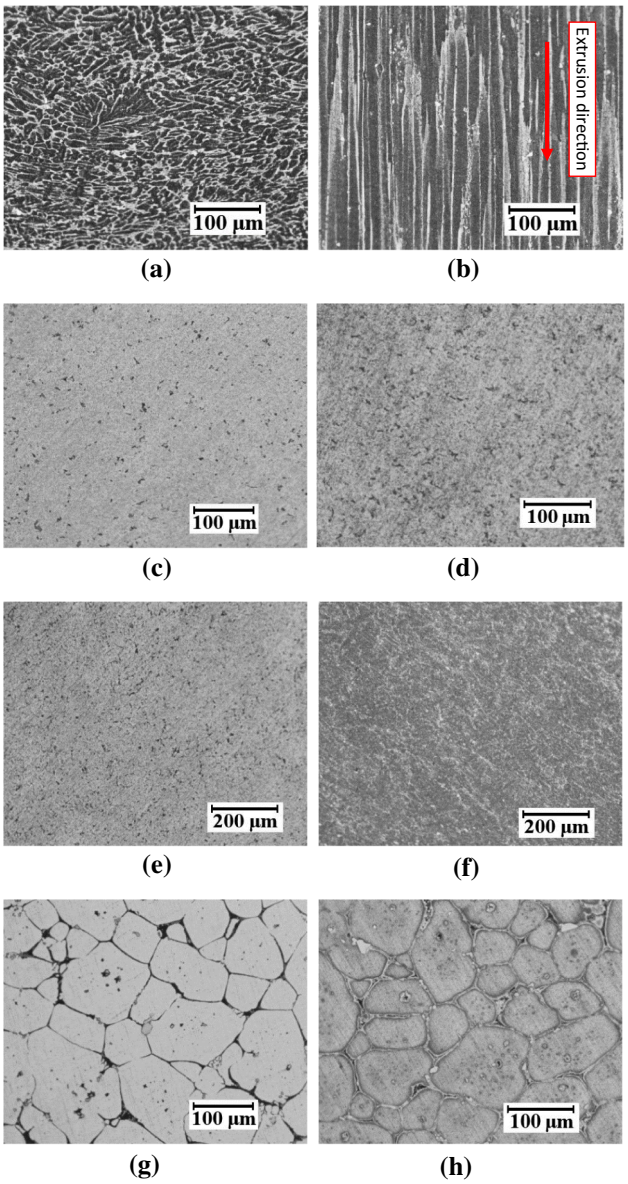

Fig. 7 Optical micrographs of the samples etched with different solutions. **a** Perpendicular to the extrusion direction; **b**–**h** parallel to the extrusion direction. **a** T0, Weck's, 6 s etching, 200× **b** T0, Weck's, 6 s etching, 200× **c** T0, Keller's, 15 s etching, 200× **d** T0, 10% NaOH, 30 s etching, 200× **e** T0, macro etching, 30 s etching, 100× **f** T0, Graff and Sargent, 30 s etching, 100× **g** 630 °C-25 min, Keller's, 15 s etching, 100× **h** 630 °C-25 min, Weck's, 6 s etching, 100×

deformation of the specimens which leads to recovery and recrystallization. The energy increases in direct proportion to the deformation ratio, which promotes the microstructural transition from dendritic to spheroidal grains and creates a decent strain induced effect.

During isothermal heat treatment, recrystallization takes place and the liquid wets the recrystallized high angle grain boundaries. The first liquid is in tendency to occur at grain boundaries because these areas have high solute concen-

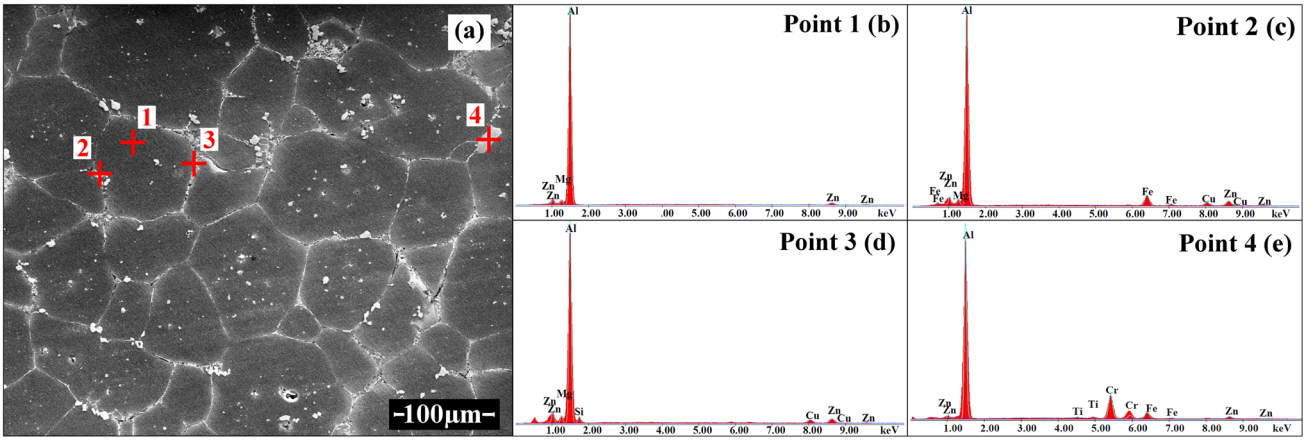

Fig. 8 SEM image of the sample held at 630 °C for 25 min (**a**) and EDS analyses of main phase and secondary phases present at the grain boundaries (**b**–**e**)

trations and low melting points. Resulting microstructure consists of α-Al solid grains surrounded by liquid phase and some entrapped liquid phases inside the solid grains.

The energy-dispersive spectras shown in Fig. 8 present higher levels of Zn, Fe, and Cu in the boundary phases appearing as white areas (Point 2) and increased levels of Mg, Zn, Si, Cu appearing as black areas (Point 3). The solid grains consist of Al and small amounts of Zn and Mg (Point 1) and are deprived of Si and Cu as a result of the microsegregation of these elements at the boundaries of the grains. The segregation of Cu and Si causes the melting temperature of the solid grains to increase and the melting temperature at grain boundaries to decrease and leads the formation of liquid phase around the solid grains. The energy-dispersive spectra of rectangular shaped Al–Fe–Cr intermetallic particle present at the grain boundary (Point 4) are depicted in Fig. 8e.

From 20 min at 620 °C, spheroidal grains began to form. Thin film-shaped secondary phases at the grain boundaries at 25 min (Fig. 9c) broadened as the solid grains started to melt around the grain boundaries in 35–40 min (Fig. 9e, f) and the liquid phase amount increased together with increasing duration. It can be seen that longer isothermal heat treatment duration makes the grains more spheroidal while reducing the grain size dispersion but mean size of the spheroidal grains increases. Coalescence is thought to be the principal mechanism for grain growth during isothermal heat treatment as shown in the Fig. 9e. Also, the intragranular liquid entrapments in solid particles (Fig. 9f) coarsened with time. Bolouri [20] claims that these liquid phases arise from the chemical inhomogeneities of the alloy. Small intragranular liquid phases next to each other progressively merge by coalescence and some of them migrate to bigger liquid areas by diffusion with Ostwald ripening mechanism. Therefore, as the volume of secondary phase increases, the resulting microstructure becomes eutectic that leads to heterogeneous microstructure with increased anisotropic properties. At the samples held at 630 °C, starting from 15–20 min spheroidal grains are beginning to form and with increasing duration the ratio of the melt secondary and eutectic phases around the grain boundaries increases (Fig. 10).

It was observed that the liquid fraction of the semisolid material increased very much at 620 °C for 40 min and 630 °C for 35 min, and thereafter, the shape deteriorated and the specimen became mechanically incapable (Figs. 11, 12).

Higher isothermal heat treatment temperature decreases the solid volume fraction and accelerates the transformation of spheroidal grains. The relationship between grain size, form factor, solid fraction and isothermal heat treatment duration is shown in Figs. 13 and 14.

Brinell hardness measurements were taken from five different regions of the samples examined for microstructures, and averages were taken. Figures 15 and 16 show the time-varying graphs of the hardness of the specimens subjected to heat treatment. Hardness measurements and microstructural analyses are congruent. It is seen that when spheroidal grains start to form, hardness drops rapidly, and then, with the grain growth, hardness continues to fall slowly. According to Chayong [32], precipitation of transitional phases during isothermal heat treatment causes lower hardness values of specimens with spheroidal grain structure. A decrease in the hardness seems to be an undesirable feature, but it is an advantage because it will enhance the ability to be shaped during thixoforging. Hence, the material with homogeneous spheroidal grain structure produced by the SIMA process is used as raw material for the semisolid forming processes and the hardness is increased by precipitation hardening heat treatments after forming.

As a result of microstructure studies and hardness measurements, it was determined that the optimum microstruc-

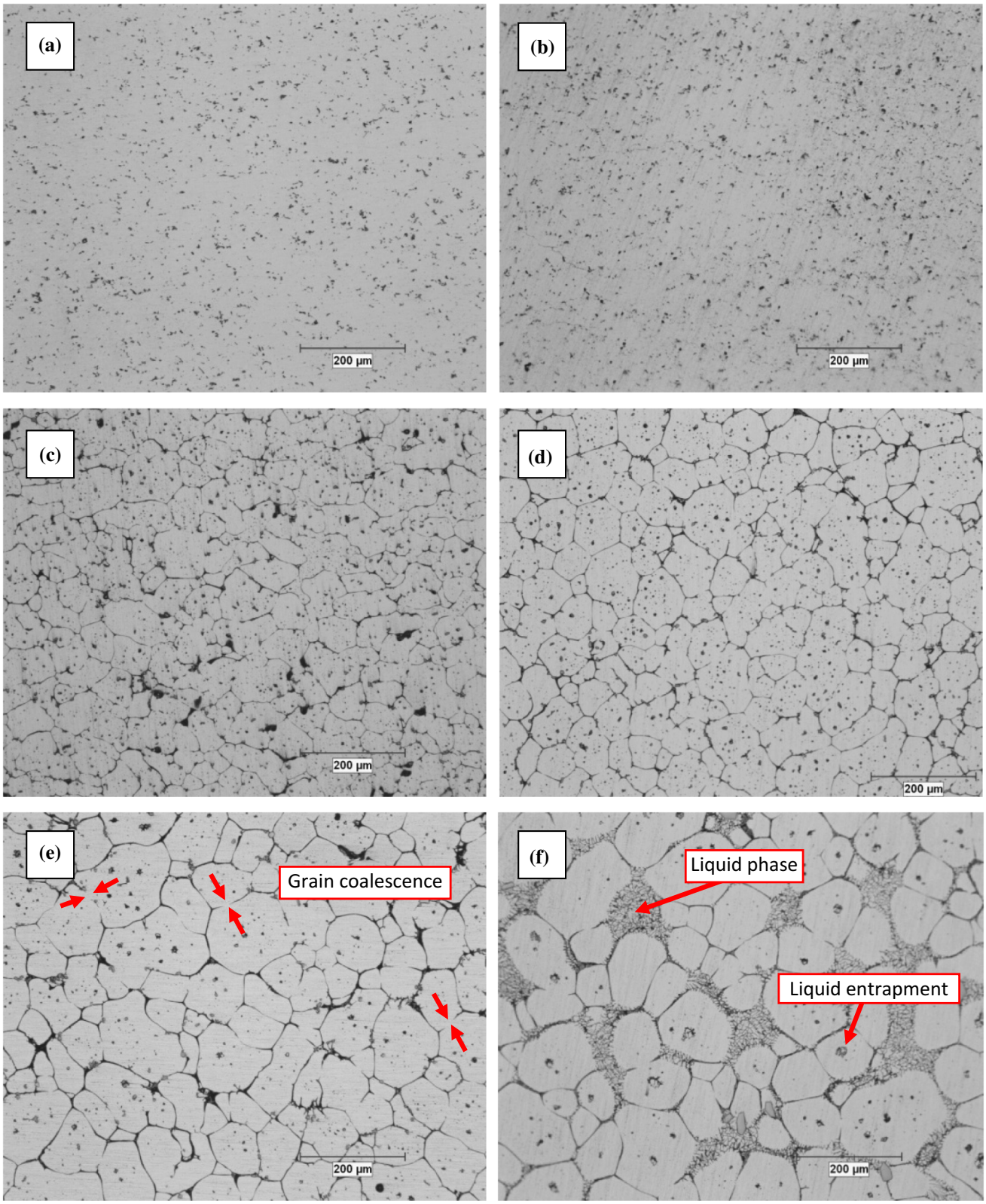

Fig. 9 Optical micrographs of the samples held at 620 °C for **a** 15 min, **b** 20 min, **c** 25 min, **d** 30 min, **e** 35 min, **f** 40 min

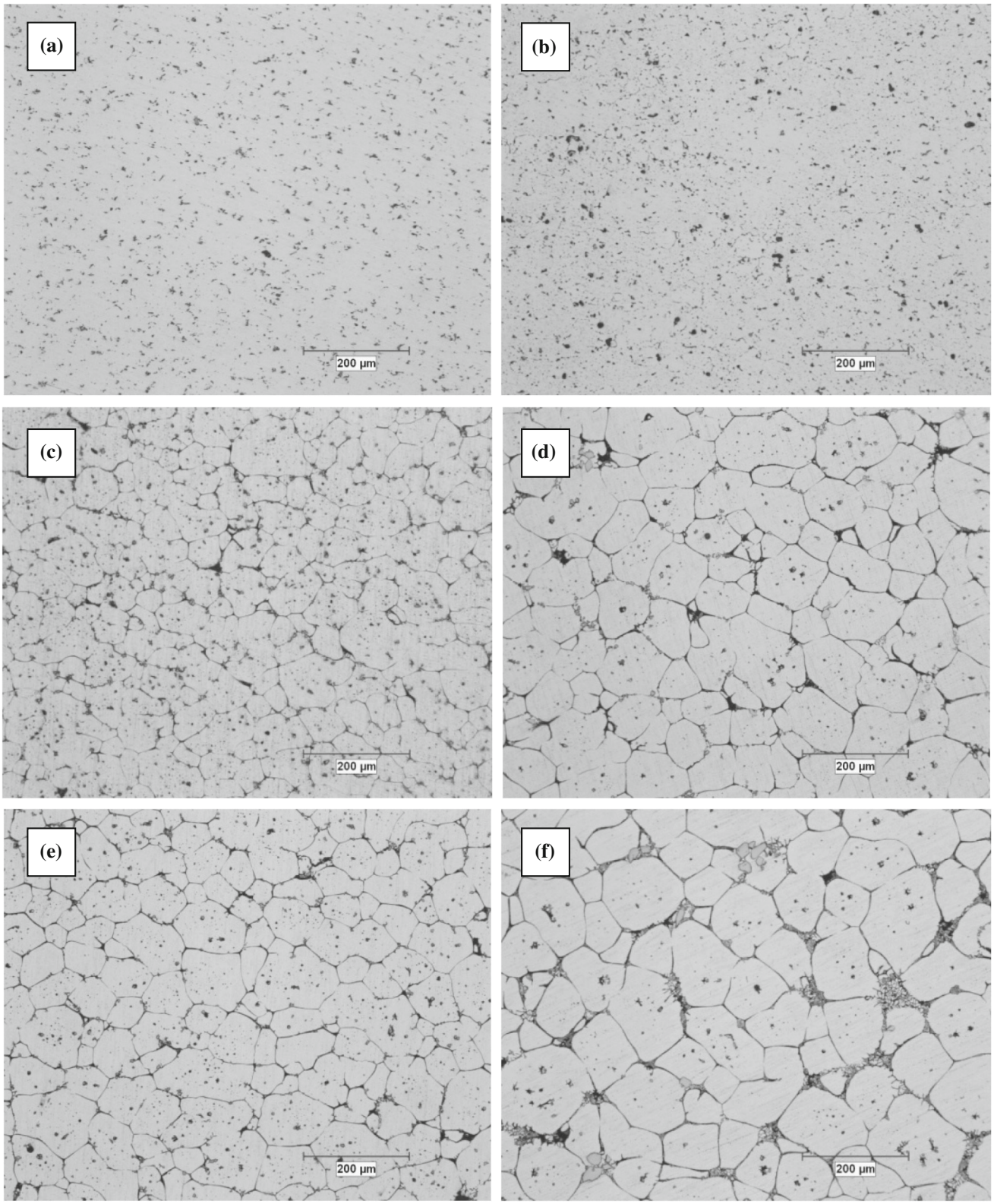

Fig. 10 Optical micrographs of the samples held at 630 °C for **a** 10 min, **b** 15 min, **c** 20 min, **d** 25 min, **e** 30 min, **f** 35 min

Fig. 11 Samples held at 620 °C for 5, 10, 15, 20, 25, 30, 35, 40, 45 min (left to right, respectively)

Fig. 12 Samples held at 630 °C for 5, 10, 15, 20, 25, 30, 35, 40 min (left to right, respectively)

ture for SIMA process is obtained at 630 °C at 25 min considering spheroidization, liquid fraction, grain size and processing time. Tensile tests were carried out after isothermal heat treatment (630 °C for 25 min) and T6 heat treatment (solutionizing at 490 °C for 45 min, quenching in water at 20 °C and aging at 120 °C for 48 h). Fifteen samples were tested, and average results were calculated. The yield strength values obtained as a result of tensile tests are given in Fig. 17. The yield strength of the samples subjected to isothermal heat treatment and aging increased to an average of 564 MPa, while the non-heat-treated samples had an average yield strength of 225 MPa. Approximately two times difference is noticeable. This relationship, which is seen in

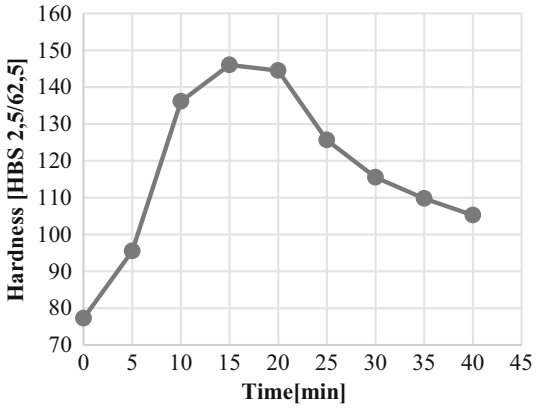

Fig. 15 Change in hardness of samples isothermal heat-treated at 620 °C over time

Fig. 13 Relationship between grain size, form factor, solid fraction and isothermal holding time at 620 °C

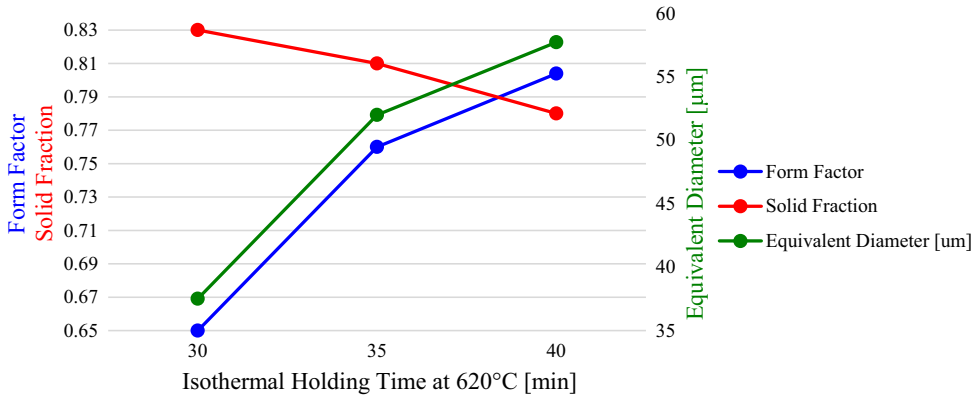

Fig. 14 Relationship between grain size, form factor, solid fraction and isothermal holding time at 630 °C

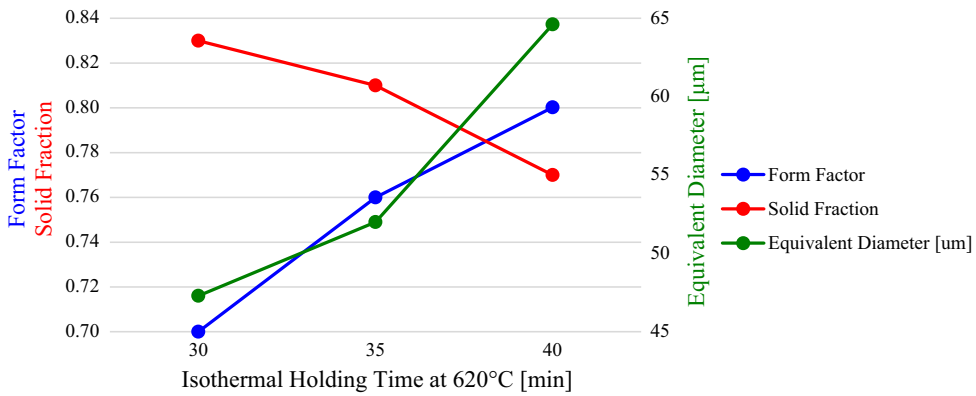

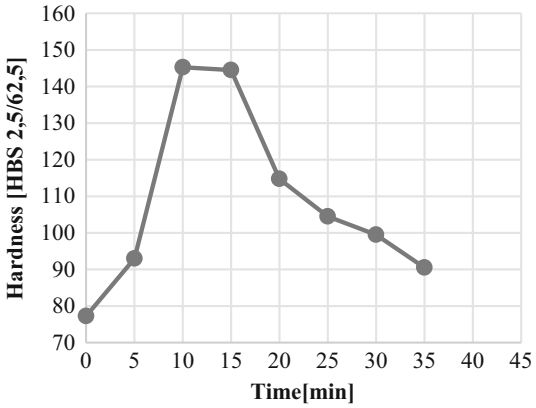

Fig. 16 Change in hardness of samples isothermal heat-treated at 630 °C over time

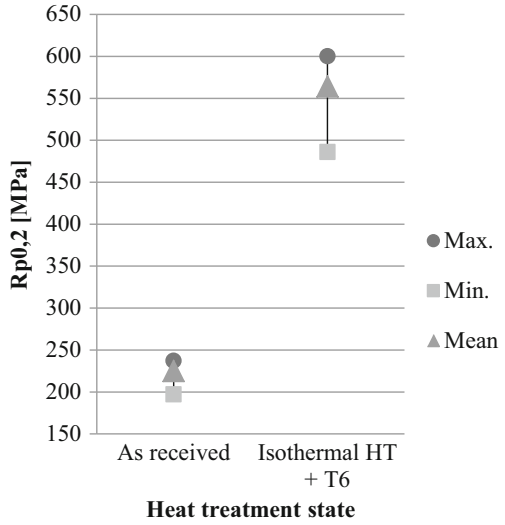

Fig. 17 Yield strength values obtained before and after heat treatments

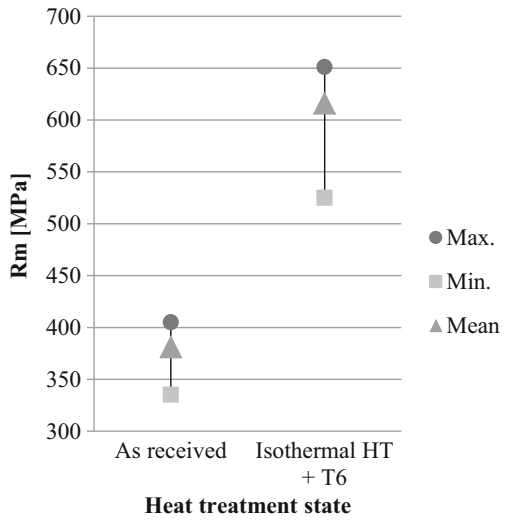

Fig. 18 Tensile strength values obtained before and after heat treatments

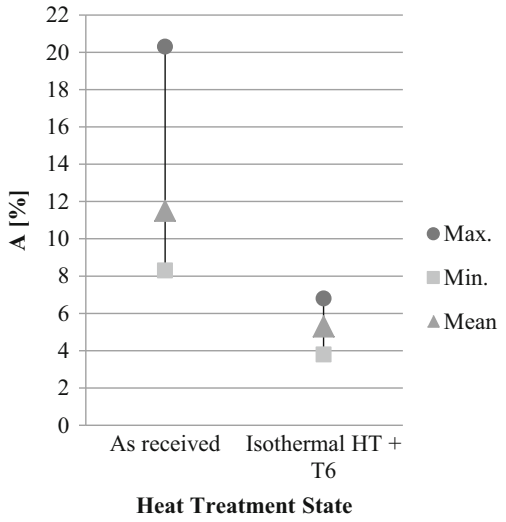

Fig. 19 Elongation values obtained before and after heat treatments

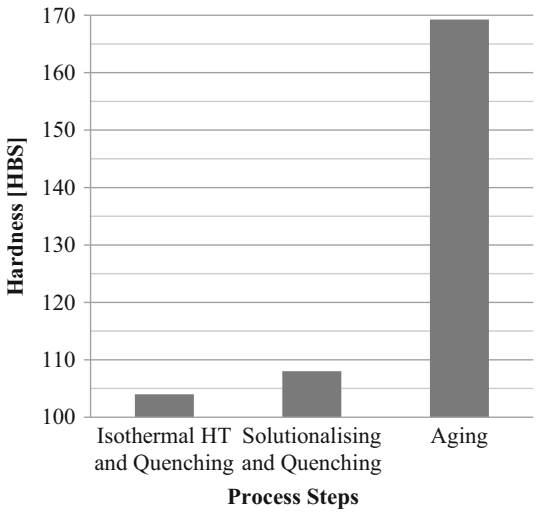

Fig. 20 Evaluation of hardness after heat treatments

yield strengths, is likewise seen in tensile strength values. As shown in Fig. 18, the average tensile strength of the samples subjected to isothermal heat treatment and aging was calculated as 615 MPa, while the average tensile strength of the samples without heat treatment was 381 MPa. The exact opposite of this relation in strength values is determined in values of elongation at break. In the samples subjected to the aging treatment, the values of the elongation at break decreased significantly (Fig. 19). Evaluation of hardness after heat treatments is given in Fig. 20.

These values are close to the mechanical properties of wrought 7075-T6. While hardness, tensile and yield strengths of isothermal heat-treated 7075 alloy in T6 condition comply with the expected properties of wrought 7075-T6 alloy, just elongation is decreased after the process. Table 3 shows the

Table 3 Mechanical properties of 7075-T6 alloy [33]

Rm (MPa)	$Rp_{0.2}$(MPa)	A (%)	Hardness (HB)
572	503	11	150

mechanical properties of wrought 7075-T6 alloy for comparison.

4 Conclusions

Semisolid forming is a relatively new technology that can be counted on to produce high-quality aluminum parts with less process steps and complex shape. Aluminum alloys are required to have homogeneous spheroidal grain structure in order to be able to be formed in semisolid state. The aim of this work is to assess the effect of isothermal heat treatment parameters on the microstructural and mechanical properties of 7075 alloy and to determine the optimum process parameters for the equiaxed spheroidal grain structure with reasonable solid/liquid ratio. In this work, it is seen that:

- The desired spheroidal grain structure can be obtained by applying SIMA process to commercially available extruded and stretched 7075 Al alloy material.
- During the reheating to the semisolid temperature, after 40 min at 620 °C and after 35 min at 630 °C, the liquid ratio of the semisolid material increases too much and becomes mechanically unstable.
- From 20 min at 620 °C spheroidal grains are beginning to form. At 35–40 min, the liquid ratio increases excessively.
- From 15–20 min at 630 °C, spheroidal particles are beginning to form and from 30 to 35 min, the liquid ratio increases excessively.
- Longer isothermal heat treatment duration makes the semisolid grains more spheroidal, but the mean size of the grains increases.
- Higher isothermal temperature results in a lower solid volume fraction and accelerated spheroidal transition.
- The reheating temperature and holding time are of great importance for the semisolid forming processes. At higher temperatures, spheroidization increases and required holding time decreases, but at the same time, the appropriate time interval of spheroidal grains is also narrows. Therefore, the temperature and isothermal holding time must be precisely controlled during the reheating phase to the semisolid temperature.
- As a result of microstructural analysis and mechanical tests, it was determined that the optimum microstructure for SIMA process is obtained at 630 °C at 25 min considering spheroidization, liquid fraction, grain size and processing time.
- Subsequent T6 heat treatment resulted in mechanical properties close to those of 7075 alloy in the wrought T6 heat-treated condition. 564 MPa yield strength, 616 MPa tensile strength and 5.3% elongation are achieved.

Acknowledgements This work was supported by Pamukkale University Scientific Research Projects Fund (PAUBAP), Project No. 2011FBE088.

References

1. Farzadi, A.; Bahmani, M.; Haghshenas, D.F.: Optimization of operational parameters in friction stir welding of AA7075-T6 aluminum alloy using response surface method. Arab. J. Sci. Eng. **42**, 4905–4916 (2017). https://doi.org/10.1007/s13369-017-2741-6
2. Zou, X.L; Yan, H.; Chen, X.H.: Evolution of second phases and mechanical properties of 7075 Al alloy processed by solution heat treatment. Trans. Nonferrous Met. Soc. China (English Ed. 27, 2146–2155 (2017). https://doi.org/10.1016/S1003-6326(17)60240-1
3. Yildirim, M.; Özyürek, D.; Gürü, M.: The effects of precipitate size on the hardness and wear behaviors of aged 7075 aluminum alloys produced by powder metallurgy route. Arab. J. Sci. Eng. **41**, 4273–4281 (2016). https://doi.org/10.1007/s13369-016-2078-6
4. Sun, Y.; Jiang, F.; Zhang, H.; Su, J.; Yuan, W.: Residual stress relief in Al–Zn–Mg–Cu alloy by a new multistage interrupted artificial aging treatment. Mater. Des. **92**, 281–287 (2016). https://doi.org/10.1016/j.matdes.2015.12.004
5. Subramanian, M.; Sakthivel, M.; Sudhakaran, R.: Modeling and analysis of surface roughness of AL7075-T6 in end milling process using response surface methodology. Arab. J. Sci. Eng. **39**, 7299–7313 (2014). https://doi.org/10.1007/s13369-014-1219-z
6. Cong, F.G.; Zhao, G.; Jiang, F.; Tian, N.; Li, R.F.: Effect of homogenization treatment on microstructure and mechanical properties of DC cast 7X50 aluminum alloy. Trans. Nonferrous Met. Soc. China (English Ed. 25, 1027–1034 (2015). https://doi.org/10.1016/S1003-6326(15)63694-9
7. Ketabchi, M.; Mohammadi, H.; Izadi, M.: Finite-element simulation and experimental investigation of isothermal backward extrusion of 7075 Al alloy. Arab. J. Sci. Eng. **37**, 2287–2296 (2012). https://doi.org/10.1007/s13369-012-0320-4
8. Liu, T.; He, C.; Li, G.; Meng, X.; Shi, C.; Zhao, N.: Microstructural evolution in Al–Zn–Mg–Cu–Sc–Zr alloys during short-time homogenization. Int. J. Miner. Metall. Mater. **22**, 516–523 (2015). https://doi.org/10.1007/s12613-015-1101-3
9. Vinarcik, E.J.: High Integrity Die Casting Processes. Wiley (2002). https://www.wiley.com/en-us/High+Integrity+Die+CastingProcesses-p-9780471275466
10. Altan, T.; Ngaile, G.: In: Altan T, Ngaile G, Shen G (eds) Cold and Hot Forging: Fundamentals and Applications. ASM International (2005). https://www.asminternational.org/search/-/journal_content/56/10192/05104G/PUBLICATION
11. Thixoforming: Semi-solid Metal Processing" Editor: Hirt G, Kopp R, Wiley (2009). https://www.wiley.com/en-us/Thixoforming%3A+Semi+solid+Metal+Processing-p-9783527623976
12. Atkinson, H.V.; Burke, K.; Vaneetveld, G.: Recrystallisation in the semi-solid state in 7075 aluminium alloy. Int. J. Mater. Form. **1**, 973–976 (2008). https://doi.org/10.1007/s12289-008-0220-z

13. Flemings, M.C.; Riek, R.G.; Young, K.P.: Rheocasting. Mater. Sci. Eng. **25**, 103–117 (1976). https://doi.org/10.1016/0025-5416(76)90057-4
14. Guo, H.; Yang, X.; Wang, J.; Hu, B.; Zhu, G.: Effects of rheoforming on microstructures and mechanical properties of 7075 wrought aluminum alloy. Trans. Nonferrous Met. Soc. China (English Ed. 20, 355–360 (2010). https://doi.org/10.1016/S1003-6326(09)60146-1
15. Young, K.P.; Kyonka, C.P.; Courtois, J.A.: Fine grained metal composition. https://patents.google.com/patent/US4415374 (1983)
16. Fu, J.-L.; Jiang, H.-J.; Wang, K.-K.: Influence of processing parameters on microstructural evolution and tensile properties for 7075 Al alloy prepared by an ECAP-based SIMA process. Acta Metall. Sin. (English Lett. (2017). https://doi.org/10.1007/s40195-017-0672-6
17. Chayong, S.; Atkinson, H.V.; Kapranos, P.: Thixoforming 7075 aluminium alloys. Mater. Sci. Eng. A **390**, 3–12 (2005). https://doi.org/10.1016/j.msea.2004.05.004
18. Rikhtegar, F.; Ketabchi, M.: Investigation of mechanical properties of 7075 Al alloy formed by forward thixoextrusion process. Mater. Des. **31**, 3943–3948 (2010). https://doi.org/10.1016/j.matdes.2010.03.032
19. Sang-Yong, L.; Jung-Hwan, L.; Young-Seon, L.: Characterization of Al 7075 alloys after cold working and heating in the semi-solid temperature range. J. Mater. Process. Technol. **111**, 42–47 (2001). https://doi.org/10.1016/S0924-0136(01)00494-0
20. Bolouri, A.; Shahmiri, M.; Cheshmeh, E.N.H.: Microstructural evolution during semisolid state strain induced melt activation process of aluminum 7075 alloy. Trans. Nonferrous Met. Soc. China (English Ed. 20, 1663–1671 (2010). https://doi.org/10.1016/S1003-6326(09)60355-1
21. Neag, A.; Favier, V.; Bigot, R.; Pop, M.: Microstructure and flow behaviour during backward extrusion of semi-solid 7075 aluminium alloy. J. Mater. Process. Technol. **212**, 1472–1480 (2012). https://doi.org/10.1016/j.jmatprotec.2012.02.003
22. Binesh, B.; Aghaie-Khafri, M.: Microstructure and texture characterization of 7075 Al alloy during the SIMA process. Mater. Charact. **106**, 390–403 (2015). https://doi.org/10.1016/j.matchar.2015.06.013
23. Jiang, J.; Wang, Y.; Xiao, G.; Nie, X.: Comparison of microstructural evolution of 7075 aluminum alloy fabricated by SIMA and RAP. J. Mater. Process. Technol. **238**, 361–372 (2016). https://doi.org/10.1016/j.jmatprotec.2016.06.020
24. Meshkabadi, R.; Faraji, G.; Javdani, A.; Pouyafar, V.: Combined effects of ECAP and subsequent heating parameters on semi-solid microstructure of 7075 aluminum alloy. Trans. Nonferrous Met. Soc. China (English Ed. 26, 3091–3101 (2016). https://doi.org/10.1016/S1003-6326(16)64441-2
25. Li, M.; Li, Y.; Bi, G.; Huang, X.; Chen, T.; Ma, Y.: Effects of melt treatment temperature and isothermal holding parameter on water-quenched microstructures of A356 aluminum alloy semisolid slurry. Trans. Nonferrous Met. Soc. China (English Ed. 28, 393–403 (2018). https://doi.org/10.1016/S1003-6326(18)64673-4
26. Zhou, B.; Kang, Y.L.; Zhu, G.M.; Gao, J.Z.; Qi, M.F.; Zhang, H.H.: Forced convection rheoforming process for preparation of 7075 aluminum alloy semisolid slurry and its numerical simulation. Trans. Nonferrous Met. Soc. China (English Ed. 24, 1109–1116 (2014). https://doi.org/10.1016/S1003-6326(14)63169-1
27. Kılıclı, V.; Akar, N.; Erdogan, M.; Kocatepe, K.: Tensile fracture behavior of AA7075 alloy produced by thixocasting. Trans. Nonferrous Met. Soc. China (English Ed. 26, 1222–1231 (2016). https://doi.org/10.1016/S1003-6326(16)64223-1
28. Yan, G.; Zhao, S.; Ma, S.; Shou, H.: Microstructural evolution of A356.2 alloy prepared by the SIMA process. Mater. Charact. **69**, 45–51 (2012). https://doi.org/10.1016/j.matchar.2012.04.005
29. Mohammadi, H.; Ketabchi, M.; Kalaki, A.: Microstructural evolution and mechanical properties of back-extruded Al 7075 alloy in the semi-solid state. Int. J. Mater. Form. **5**, 109–119 (2012). https://doi.org/10.1007/s12289-010-1022-7
30. Gecu, R.; Acar, S.; Kısasoz, A.; Altug Guler, K.; Karaaslan, A.: Influence of T6 heat treatment on A356 and A380 aluminium alloys manufactured by thixoforging combined with low superheat casting. Trans. Nonferrous Met. Soc. China (English Ed. 28, 385–392 (2018). https://doi.org/10.1016/S1003-6326(18)64672-2
31. Zhang, Q.Q.; Cao, Z.Y.; Zhang, Y.F.; Su, G.H.; Liu, Y.B.: Effect of compression ratio on the microstructure evolution of semisolid AZ91D alloy. J. Mater. Process. Technol. **184**, 195–200 (2007). https://doi.org/10.1016/j.jmatprotec.2006.11.022
32. Thixoforming Processing of Aluminium 7075 Alloy, Ph.D. Thesis, University of Sheffield (2002). http://ethos.bl.uk/OrderDetails.do?uin=uk.bl.ethos.251217
33. ASM International: ASM Handbook Volume 2 Properties and Selection: Nonferrous Alloys and Special-Purpose Materials. (2001)